DOI: 10.1111/jbi.13189

ORIGINAL ARTICLE

WILEY Journal of Biogeography

The contribution of neutral evolution and adaptive processes in driving phenotypic divergence in a model mammalian species, the Andean fox *Lycalopex culpaeus*

Pablo A. Martinez[1,2] | Monica V. Pia[3] | Ilham A. Bahechar[4] | Wagner F. Molina[1] | Claudio J. Bidau[5] | Juan I. Montoya-Burgos[4]

[1]Department of Cell Biology and Genetics, Biosciences Center, Universidade Federal do Rio Grande do Norte, Rio Grande do Norte, Brazil

[2]PIBi-Lab, Laboratorio de Pesquisas Integrativas em Biodiversidade, Departament of Biology, Universidade Federal de Sergipe, Avenida Marechal Rondon, São Cristóvão, Sergipe, Brazil

[3]Department of Biostatistics, Córdoba National University, Córdoba, Argentina

[4]Department of Genetics and Evolution, University of Geneva, Geneva, Switzerland

[5]Paraná y Los Claveles 3304, Garupá, Misiones, Argentina

Correspondence
Juan I. Montoya-Burgos, Department of Genetics and Evolution, University of Geneva, Geneva, Switzerland.
Email: juan.montoya@unige.ch

Funding information
Coordenação de Aperfeiçoamento de Pessoal de Nível Superior; FNS, Grant/Award Number: 31003A_141233; CAPES-REUNI; PE Course of UFRN; Claraz Donation

Editor: Aristeidis Parmakelis

Abstract

Aim: Understanding the mechanisms that drive phenotypic divergence along climatic gradients is a long-standing goal of biogeography. To fulfil this objective, we tested if neutral and/or adaptive effects drive phenotypic diversification. We quantified the effects of neutral evolution and natural selection on morphological variability of a well-suited mammalian species, the fox, *Lycalopex culpaeus*.

Location: South America.

Methods: We analysed variations in skull shape, jaw shape and skull size in *L. culpaeus*. The processes underlying our models were: local adaptation, and short- or long-term neutral evolution. We inferred genetic population structure using mitochondrial and nuclear markers, we quantified morphological differences among populations by performing geometric morphometric analyses, and we inferred an ecological niche model for calculating environmental resistance between populations.

Results: We identified six genetically differentiated populations of the Andean fox, which correspond well to the described subspecies. We showed that skull shape variation is explained by population structure. Skull size showed a clear Bergmannian pattern with larger animals in higher latitudes (in absolute values). Skull size divergence is driven by the combined effects of environmental factors and population structure. Intriguingly, none of the models explains the variation observed in jaw shape.

Main Conclusion: Population phenotypic variation in the Andean fox *L. culpaeus* is driven by deterministic and neutral processes. The methodological framework presented here opens up new opportunities to study phenotypic evolution; it allowed us to demonstrate that the processes explaining trait variation can differ among traits and to show empirically for the first time that a trait can diverge among populations due to simultaneous adaptation and neutral evolution.

KEYWORDS
ecology, environment, multiple regression, natural selection, niche modelling, phenotypic evolution, population genetics

1 | INTRODUCTION

Deciphering the causes of phenotypic divergence among populations and species is a fundamental goal of evolutionary biology (Fisher, 1930). Although increasing evidence links neutral evolutionary rate with adaptive evolution at the molecular level (Montoya-Burgos, 2011; Wagner, 2008), the relationships between neutral and adaptive processes and their relative role in driving intraspecific phenotypic variation are still poorly understood. Phenotypic differentiation among populations is thought to be caused by genetic and/or environmental factors that can be classified into selective processes, including natural and sexual selection, or neutral processes (Mitchell-Olds, Willis, & Goldstein, 2007). Also, genetic and non-genetic maternal effects can affect the response of individuals to natural and sexual selection, potentially favouring population divergence (Mousseau, Uller, Wapstra, & Badyaev, 2009).

When considering the genetic determinants of the phenotype, local phenotypic characteristics can be produced through the action of neutral evolution, sexual selection, divergent selection or a combination of these processes. Importantly, divergent selection, which acts in contrasting directions in two or more populations (Rundle & Nosil, 2005), can lead to local adaptation, where individuals bear traits that are advantageous under the local conditions of their populations. These processes either control or depend on the level of gene flow among populations. High gene flow will reduce or inhibit local phenotypic divergence by causing the dilution of the genotypes responsible for local phenotypic characteristics as well as the introduction of genotypes encoding different phenotypes (North, Pennanen, Ovaskainen, & Laine, 2011). However, gene flow can be restricted in several ways: geographical barriers, low species vagility, pre-zygotic barriers such as changes in sexual behaviour that prevent mating or post-mating incompatibilities leading to selection against hybrids or their formation (Wang & Summers, 2010).

Environmental factors can also lead to local phenotypic characteristics, either as a result of phenotypic plasticity or of local adaptation (Davis, Shaw, & Etterson, 2005). The phenotypic response to these two processes will depend on the time-scale considered, on the life history of the species, and on the rate and extent of environmental change (Meyers & Bull, 2002). Moreover, inter-population phenotypic divergence may result from the action of a single driving force or through the combination of various forces. Thus, the explanatory factors that contribute to geographical phenotypic divergence are only partially known for a limited number of species (e.g. beach mice (*Peromyscus polionotus*) by Mullen, Vignieri, Gore, & Hoekstra, 2009; poison-dart frog (*Dendrobates pumilio*) by Wang & Summers, 2010).

We have investigated the determinants that drive intraspecific phenotypic divergence in mammals using a canid representative as a model system. Canidae is a family that offers good model species, first because the current group (subfamily Caninae) underwent a high diversification rate in the last 8 million years (Slater, 2015; Wayne et al., 1997). Second, many canid species display wide distributional ranges encompassing several ecoregions, with many local eco-morphotypes (Zurano, Martinez, Hernández, Montoya-Burgos, & Costa, 2017). Demonstrative examples are the grey wolf and red fox which have the widest distributional ranges among all extant mammals with tens of geographical morphotypes (Wozencraft, 2005). Among canid species, the Andean fox *Lycalopex culpaeus* Molina, 1782 is distinctive due to its wide latitudinal distribution, which ranges from southern Colombia to Cape Horn (Novaro, 1997). The distribution encompasses an outstanding variety of ecoregions (Figure 1), with environmental variation that might have triggered local adaptive changes. Six subspecies are recognized (Wozencraft, 2005), with distributional ranges continuous along the Andes bar one exception, i.e. the disjunct distribution of *L. c. smithersi* in the mountain range of Córdoba, Argentina (Figure 1).

Subspecies of the Andean fox vary in adult body size, cranial traits and colour pattern (Wozencraft, 2005). In mammals, these traits typically vary among populations and the underlying causes are often subject to debate. In particular, body size has been shown to increase with increasing latitude, a correlation referred to as Bergmann's rule (Bergmann, 1847). This rule has been initially interpreted as an adaptation to temperature, with a lower surface-to-volume ratio limiting heat loss in cold regions and a higher ratio favouring heat dissipation in warm areas (Mayr, 1956). However, body size change with latitude could be a response to primary productivity and food availability (Rosenzweig, 1968), two variables often correlated with latitude.

We used the Andean fox as a model mammalian system, for which we characterized three phenotypic traits: skull shape, jaw shape and skull size, the latter as a proxy for body size. We analysed if the phenotypic divergence among populations is driven by the genetic structure of populations and/or climatic factors. We tested the hypothesis that climatic factors are associated with skull and jaw shapes (functionality hypothesis). We expect this because, in carnivores, the shapes of the skull and jaw are strongly associated with the function and force of the bite of species (Figueirido, Tseng, & Martín-Serra, 2013). Thus, clinal climatic variation could be associated to changes in the amount and kind of available food items driving the divergence of skull and jaw shape between populations. On the other hand, we tested if body size is associated with temperature (thermoregulation hypothesis) and/or resource availability (resource hypothesis). Finally, the size and shape of anatomical structures can also be driven by neutral processes. Thus, we tested the hypothesis that population structure determines size and shape in *L. culpaeus* (neutral hypothesis). To achieve our goals, we first inferred the population structure of the species based on mitochondrial and nuclear markers. We also modelled the ecological niche of the species to measure environmental resistance among populations.

2 | MATERIALS AND METHODS

2.1 | Genetic data acquisition

Skin tissue samples of 62 *L. culpaeus* individuals were obtained from institutional or museum collections, or taken from skins belonging to

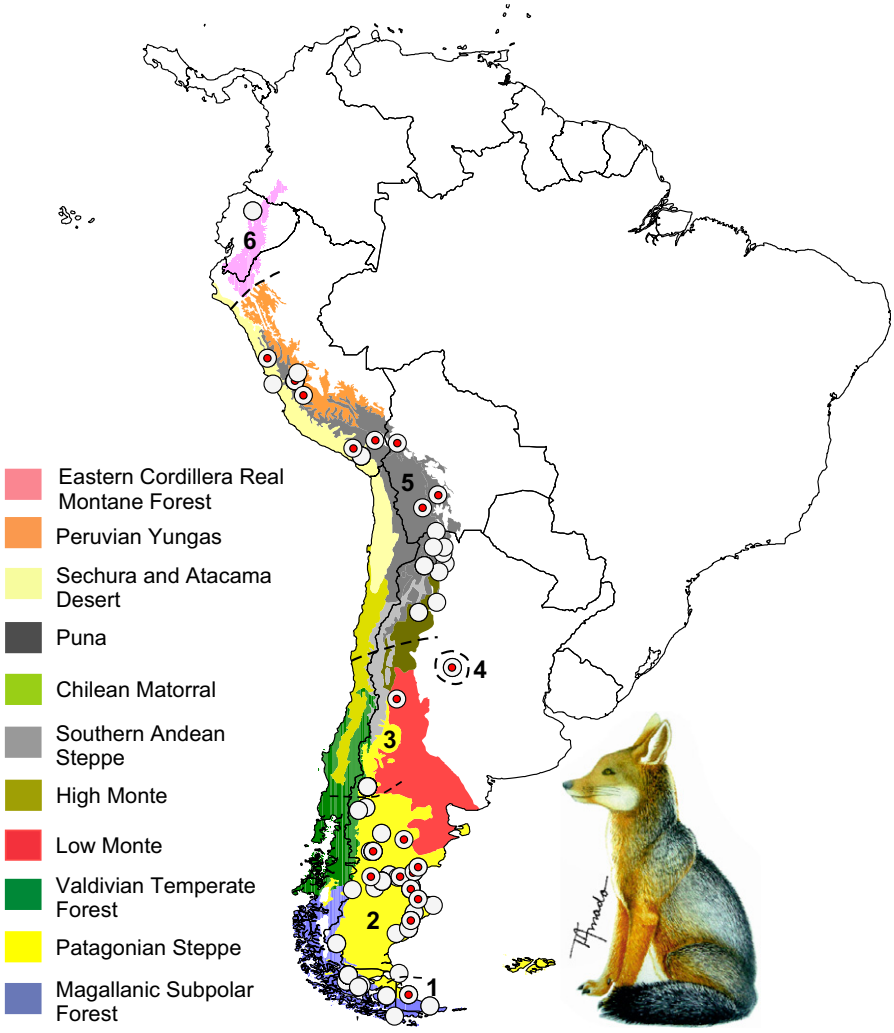

FIGURE 1 Distributional range of the Andean fox *Lycalopex culpaeus* with the ecoregions it encompasses and the sampling localities. The dotted lines separate the different subspecies: *L. c. lycoides* (1); *L. c. magellanica* (2); *L. c. culpaeus* (3); *L. c. smithersi* (4); *L. c. andina* (5); *L. c. reissii* (6). The distributional range is continuous from southern Colombia to Tierra del Fuego, with the exception of the isolated mountain range of Córdoba, in Argentina, which hosts the endemic subspecies *L. c. smithersi* (4). The ecoregions (Olson et al., 2001) are coloured. White circles indicate localities with morphological data and red dots show localities with genetic data. A locality can contain more than one sample

local villagers or from dead animals found along the roads, with the corresponding field and transportation official permits (Figure 1 and Table S1 in Appendix S1). After total DNA extraction, two mitochondrial markers were analysed: a fragment of COI (652 bp) and the D-loop (598 bp). To confirm the results based on mtDNA, we analysed three nuclear introns: (1) a 464 bp fragment of the fourth intron of the coiled-coil domain-containing the 90B gene (CCDC90B); (2) a 529 bp fragment of intron number 49 of the ATP-binding cassette transporter gene (ABCA1); and (3) a 345 bp fragment of intron number 20 of the protein sel-1 homologue 3 (SEL1L3) (details of the primer sequences and amplification appear in Table S2 of Appendix S1). We checked for the absence of stop codons in the COI sequences by translating them. All sequences have been deposited in GenBank (Table S1 in Appendix S1).

2.2 | Population structure and phylogenetic analyses

We performed analyses using the haplotypes obtained by concatenating the two mitochondrial markers. We determined the number of genetically and geographically homogenous populations (*K*) using SAMOVA 1.0 (Dupanloup, Schneider, & Excoffier, 2002). We tested values of *K* ranging from 2 to 6 and the best grouping scheme was identified by the *p*-value and the highest F_{ct} value. Population structure was also assessed by pairwise comparisons of the F_{st} values, as implemented in ARLEQUIN 3.5 (Excoffier & Lischer, 2010). To check whether the mtDNA-based population structure was recovered by the nuclear markers, we tested if the allelic frequencies among the populations were significantly different using a chi-squared test in GENEPOP 3.4 (Raymond & Rousset, 1995).

We performed manual DNA sequence alignment, and for each mitochondrial marker we assessed the best model of sequence evolution using PARTITIONFINDER 2 (Lanfear, Calcott, Ho, & Guindon, 2012). We established evolutionary models for the markers by alignment, considering the position of the codons for COI and treating the D-loop fragment as a single partition. We established optimum partitions with the Akaike information criterion (AIC)-based "greedy" algorithm in PARTITIONFINDER 2 (Lanfear et al., 2012). We used the best scoring model (based on AIC) that was available in the analysis software for downstream analyses. The phylogenetic relationships between mitochondrial haplotypes were reconstructed using the concatenated sequences of the mtDNA markers (1,243 bp),

partitioning by markers, using Bayesian analyses with MRBAYES 3.2.6 (Huelsenbeck & Ronquist, 2001), and maximum likelihood with RAXML 7.0 (Stamatakis, 2006) with 10 searches for every 1,000 bootstrap replicates. The inclusion of more taxon sampling provides higher resolution of the ingroup monophyly (Heath, Hedtke, & Hillis, 2008; Pollock, Zwickl, McGuire, & Hillis, 2002). Thus, we selected as outgroups two closely related species, *L. griseus* and *Cerdocyon thous*, and the more distant coyote *Canis latrans*.

2.3 | Ecological niche model, isolation by distance and environmental resistance

An ecological niche model (ENM) for *L. culpaeus* was inferred using MAXENT 3.4 (Phillips & Dudik, 2008) (more details in Appendix S1). The climatic variables were based on current environmental variables from WorldClim (Hijmans, Cameron, Parra, Jones, & Jarvis, 2005) (Table S3 in Appendix S1) and projected into the Last Glacial Maximum (LGM, 21k).

We evaluated two models of IBD: IBD based on raw geographical distances and IBD-log based on log-transformed geographical distances, following Rousset (1997). We measured the geographical distance between populations as distance between the geographical centroid of the sampled sites. The environmental resistance between *L. culpaeus* populations was quantified by the resistance distance calculated by the circuit theory-based model implemented in CIRCUITSCAPE 4.0.5 (Shah & McRae, 2008), using as per-cell conductance the habitat suitability score obtained by the ENM that we inferred. This method simultaneously considers the environmental cost of multiple possible paths connecting pairs of populations and calculates a weighted average of their connectivity, resulting in the resistance distance between pairs of populations (Shah & McRae, 2008). Thus, isolation-by-resistance (IBR) takes into account not only the distance between populations but also establishes a cost associated with the availability and suitability of the environment among populations. To determine which of the two models, IBD or IBR, predicts genetic differentiation the best, we first performed correlations with genetic structure (F_{st}). These tests were performed using the Mantel test with the Pearson correlation as implemented in "ecodist" (Goslee & Urban, 2007) in the R 3.2.2 (R Core Team, 2015) platform. The inter-populational genetic structure was not explained by any of the analysed IBD models (IBD: $df = 13$, $r^2 = .04$, $p = .62$; IBD-log: $df = 13$, $r^2 = .13$, $p = .76$). On the other hand, the IBR model explained a substantial and significant fraction of the genetic population structure ($df = 13$, $r^2 = .441$; $p = .013$). Therefore, we considered resistance distance as a predictor model for subsequent analyses instead of geographical distance.

2.4 | Measure of morphological divergence

We obtained morphological measurements for 165 skulls and 161 jaws of adult specimens of *L. culpaeus* coming from different regions of the species distributional range (Figure 1 and Table S4 in Appendix S1). Because sexual dimorphism is only subtle in this species, we analysed adult males and females jointly (Bidau & Martinez, 2016; Segura & Prevosti, 2012). We recorded 16 landmarks for the skull and 15 for the jaw (Figure S4 in Appendix S1) using the software TPSDIG2 2.16 (Rohlf, 2010). In order to avoid errors derived from the photographs, these were taken following a standardized protocol where the resting surface of the skull and mandible and that of the camera were levelled. Additionally, to minimize errors in the positioning of landmarks, all the work was done by a single researcher (PAM). To estimate the differences in the shape of the skull and the jaw between populations (as determined in our population structure analyses), we performed a full generalized Procrustes superimposition analysis, as implemented in MORPHOJ (Klingemberg, 2008) and calculated the Procrustes distances between populations using the Procrustes coordinates of all individuals belonging to each of the two populations compared. In addition, we estimated a second measure of divergence in shape from the residuals of the multivariate regression between the Procrustes coordinates and centroid size. This second approach allowed us to estimate the differences in shape independently of body size. Canonical variate analyses (CVA) allows for detecting small morphological differences between previously defined groups. Thus, to characterize the morphological differences among populations, we performed CVA using MORPHOJ (Klingemberg, 2008). As skull size is a very good proxy of body size in carnivores (Meiri, Dayan, & Simberloff, 2005), body size was estimated by the value of the centroid of the skull for each individual. Thus, given the impossibility of estimating the body mass of the individuals, skull size becomes a good proxy for body size (Fitch, 2000). To test for population differences in skull size, we performed a one-way ANOVA analysis followed by a posteriori pairwise comparisons using the Tukey post hoc test.

In most cases, we obtained the morphological and genetic data from different individuals due to the scarcity of museum specimens having both the skull and a tissue sample. However, the fact that the morphological and the genetic data characterizing a population come from different individuals is not a serious problem, as long as we can ensure that they belong to the same population (or subspecies). This assumption is based on the congruence between our genetic delineation of the populations and the morphological and distributional diagnosis of the subspecies (see Results).

2.5 | Environmental variables

We assembled a total of 23 environmental variables for the collection localities, of which 19 were taken from the WorldClim (Hijmans et al., 2005), three were extracted from Cramer and Leemans (2001) (AET [actual evapotranspiration], PET [potential evapotranspiration] and water balance), while NPP (net primary productivity) was obtained from Imhoff et al. (2004) (Table S3 in Appendix S1). The data were processed using DIVA-GIS 7.5 (Hijmans, Guarino, & Mathur, 2012). To identify the minimal set of variables that describe the environment of the areas occupied by each population (as determined in our population structure analyses), a principal components

analysis (PCA) was first performed on the correlation matrix of the environmental variables set. The "broken stick" method was then used to determine the best minimal set of variables to be included in further analyses. For each population, the values of the environmental variables were the mean values over all the sampling localities. The environmental divergence between pairs of populations was measured using the Euclidean environmental distance.

2.6 | Neutral genetic, environmental and geographical contributions to phenotypic variation

The relative contribution of population genetic structure, contemporary environmental resistance and environmental variables in explaining morphological differences among populations was analysed by establishing response matrices of inter-population distance for three phenotypic traits: (1) Procrustes distance of skull shape and Procrustes distance of skull shape independent of size, (2) Procrustes distance of jaw shape and Procrustes distance of jaw shape independent of size, and (3) Euclidean distance of skull centroid size (this measure reflects differences in skull size). We then built three explanatory matrices containing the following population pairwise distances: (1) genetic structure measured by F_{st}, (2) resistance distance and (3) Euclidean environmental distance. To identify the relative importance of the explanatory factors that correlate with the phenotypic response matrices, we performed MRM analyses with Pearson correlations, as implemented in "ecodist" (Goslee & Urban, 2007) package, in the R 3.2.2 (R Core Team, 2015) platform. All predictor variables showed a correlation <0.70, thus avoiding multicollinearity in the models (Table S5). We obtained significance values using 10,000 permutations (more details of implementation of MRM in Appendix S1). We tested all possible combinations of the explanatory variables and the best explanatory models were determined according to their significance values and their AIC scores. When two models had a ΔAIC greater than 2 units, the one with the lowest AIC was considered the best model (Burnham & Anderson, 2002).

Global patterns of geographical variation in skull size were first assessed by performing a regression between the log-transformed skull centroid size of each individual versus latitude. In order to investigate the relationships between environment and skull size, we assessed 23 environmental variables and kept a subset of nine showing the lowest correlation with the others ($r < .70$), which were the most biologically meaningful for *L. culpaeus* (Table S3 in Appendix S1). When assessing global patterns of geographical variation in skull size, spatial autocorrelation among data can lead to incorrect conclusions due to type I error. On the other hand, we analysed if climatic factors could affect skull size on a short temporal scale. Thus, to investigate further the possible influence of temperature-, precipitation- and biomass-related variables on the size of the skull, we performed an intra-lineage analysis. We selected the [Perú]+[Bolivia] lineage, corresponding to the subspecies *L. c. andina*, as it occupies the widest range of habitats while displaying a limited latitudinal distribution.

We thus computed partial or multiple simultaneous autoregressive models incorporating an autocorrelation on the covariance residuals (SAR-error method; see Kissling & Carl, 2008) between the log-transformed skull centroid size of each individual and the nine retained environmental variables, using SAM 4.0 (Rangel, Diniz-Filho, & Bini, 2010). The all-environmental variables had a variance inflation factor (VIF) less than 10 in the models, showing low multicollinearity. We selected the best models according to the AIC scores and *p*-values.

3 | RESULTS

3.1 | Population structure and haplotype phylogeny

We analysed sequences of 62 specimens of *L. culpaeus* sampled across the distribution range of the species (Figure 1 and Table S1 in Appendix S1). The population structure analysis (SAMOVA) based on the concatenated mitochondrial markers COI and D-loop indicated six highly structured populations (Table S6 in Appendix S1), named hereafter [Peru], [Bolivia], [Córdoba] (Province of Córdoba, Argentina), [Mendoza] (Province of Mendoza, Argentina), [Chubut-Santa] (Provinces of Chubut and Santa Cruz, Argentina) and [Fuego] (Province of Tierra del Fuego, Argentina) ($F_{ct} = 79.73$, $p < .001$) (Figure 2). The pairwise F_{st} values were congruent with this population delineation ($F_{st} \geq 0.29$, $p < .05$; Table 1). To give an independent support to the population structure found with the mitochondrial markers, we cloned and sequenced multiple clones of three nuclear introns for a subsample of 4–8 individuals per populations (Table S1 in Appendix S1). The analysis of the three nuclear introns indicated significant differences in allele frequencies between the populations defined by the mitochondrial markers. The only exception to this pattern was the Bolivian population that did not show significant differences with the adjacent population [Mendoza], and those from [Córdoba] and [Chubut-Santa] (Table 1, Figure 2).

Bayesian and maximum likelihood phylogenetic analysis from mitochondrial haplotypes of *L. culpaeus* showed a basal division into two main and well-supported lineages, the northern lineage including [Perú], [Bolivia] and [Córdoba], and the southern lineage grouping [Mendoza], [Chubut-Santa] and [Fuego] (Figure 2 and Figure S1 in Appendix S1). Within the northern lineage, only [Córdoba], which corresponds to the subspecies *L. c. smithersi*, showed a monophyletic group of haplotypes. Interestingly, [Perú]+[Bolivia] had intermixed haplotypes, but together they formed a monophyletic group that corresponded to the subspecies *L. c. andina*. Within the southern lineage, the haplotypes of the three populations tend to be grouped by population, yet a substantial amount of haplotypes are intermixed, revealing probable events of gene flow between populations (Figure 2 and Figure S1 in Appendix S1).

3.2 | Ecological niche model

We performed an ENM for *L. culpaeus* to assess environmental resistance between populations, one of our explanatory models. The

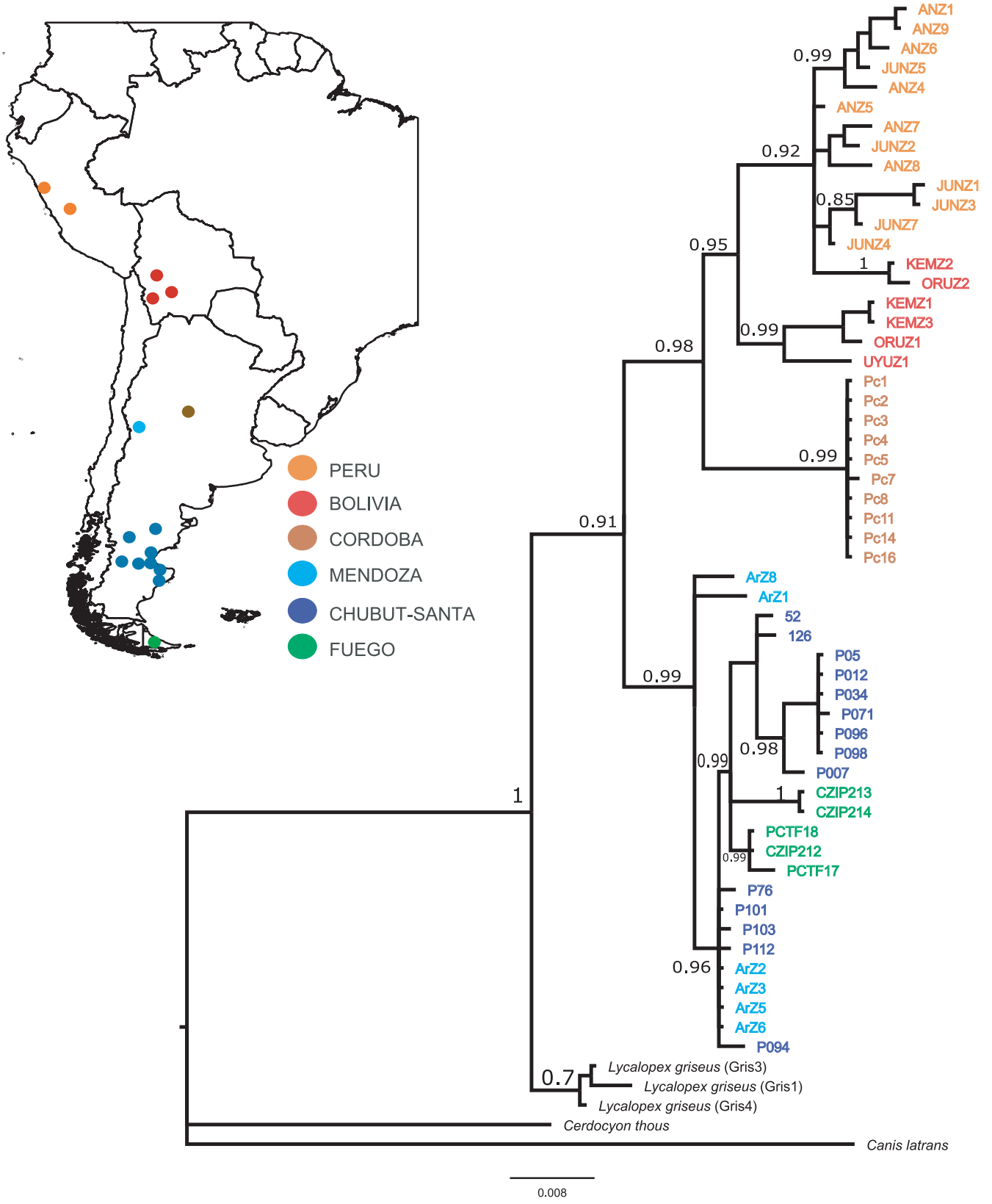

FIGURE 2 Haplotype phylogeny inferred with the Bayesian inference method based on the concatenated mitochondrial markers COI and D-loop. The best model of sequence evolution for D-loop marker is GTR+G+I and for COI is HKY+G+I according to the AICc criterion in PartitionFinder 2.1.1. Numbers above branches indicate posterior probabilities. Populations were identified using SAMOVA (Table S4)

TABLE 1 Indices of population differentiation in the Andean fox. (A) Pairwise F_{st} based on the concatenated mitochondrial markers (COI and D-loop) are shown below the diagonal; significance values are shown above the diagonal. (B) Chi-square test on pairwise difference in allele frequencies based on the three nuclear intronic markers (CCDC90B, ABCA1 and SEL1L3); chi-square values are shown below the diagonal, significance values are shown above the diagonal, with $df = 6$

	Santa-Chubut	Peru	Mendoza	Fuego	Bolivia	Cordoba
(A) Pairwise F_{st} (mtDNA)						
Santa-Chubut		***	***	***	***	***
Peru	0.78863		***	***	***	***
Mendoza	0.32594	0.74015		**	***	***
Fuego	0.36182	0.73665	0.28917		***	***
Bolivia	0.737	0.4415	0.6417	0.6021		***
Cordoba	0.9192	0.82993	0.9422	0.92429	0.744	
(B) Difference in allele frequencies based on nuclear markers						
Santa-Chubut		***	**	*	ns	***
Peru	27.08		***	**	**	***
Mendoza	16.98	23.36		***	ns	*
Fuego	14.07	22.14	24.05		*	*
Bolivia	9.86	19.06	6.9	12.2		ns
Cordoba	25.23	24.32	12.65	16.78	8.18	

*$p < .05$; **$p < .01$; ***$p < .001$; ns: not significant.

ENM itself was supported by high values of performance and accuracy (training data AUC = 0.934; test data AUC = 0.892), with a geographical projection very close to the known distributional range of this species. Remarkably, the Córdoba mountain range, which hosts the [Córdoba] population, was disconnected from the rest of the suitable habitat of the species matching its current distribution (Figure S2 in Appendix S1). From the projection into the LGM, we observed a generalized increase in the potential climatic areas for *L. culpaeus*. Interestingly enough, the population from Córdoba shows a climatic connection during LGM, with those populations from western and northwestern Argentina (Figure S2 in Appendix S1).

3.3 | Phenotypic divergence

The CVA of the skull shape resulted in a first canonical axis explaining 45.55% of the variance mainly linked to the shape of the zygomatic arch and the length of the nasal bone (Figure S3a in Appendix S1). The second axis, principally related to the size of the neurocranium, explained 26.92%. Population differences in skull shape, as estimated by Procrustes distances, were significantly different between populations with the exception of [Fuego] versus [Chubut-Santa], [Bolivia] versus [Chubut-Santa] and [Perú], and [Córdoba] versus all other populations except [Perú] (Table 2). The CVA analysis of jaw shape gave a first canonical axis explaining 41.76% of the variance (mainly related to the height of the mandibular body) (Figure S3b in Appendix S1), whereas the second axis explaining 22.7% was principally linked to the size of the coronoid and condylar processes. Jaw shape Procrustes distances were significantly different between populations with the exception of [Fuego] versus [Chubut-Santa], [Bolivia] versus [Perú] and [Córdoba] versus all other populations (Table 2). The differences observed between [Córdoba] and other populations are often large but non-significant due to the small sample size of that population ($N = 2$).

We tested for population divergence in skull size and found that most pairwise comparisons showed significant differences with the exception of: [Córdoba] versus all other populations except [Fuego]; [Bolivia] versus [Peru] and [Mendoza]; and [Peru] versus [Mendoza] (Table 2). Non-significant differences concerned essentially pairs of geographically close populations. We additionally found a positive correlation between skull size and latitude ($F = 23.88$; $n = 156$; $df = 154$; $r^2 = .13$; $p < .001$).

3.4 | Variables explaining phenotypic variation

Multiple regressions on distance matrices (MRM) were performed to identify the models explaining population variation in the phenotypic traits that we characterized. As MRM may have an excessive type I error rate when both the response and the explanatory variables display spatial autocorrelation but not when only one of these variables is affected (see Methods), we first assessed such structure and found that none of the response variables was spatially autocorrelated (Table S7 in Appendix S1). We thus avoided the problem of potentially concluding a significant association when there is none. Variation in skull shape, as the MRM results indicated, was significantly and strongly correlated with genetic structure as determined by F_{st}, with 62% of the total variation explained (Table 3). In contrast, the model combining environmental variables+resistancedistance+genetic structure (highest AIC score; Table 3) explained 75% of skull size variation. Notably, inter-population variation in jaw shape showed no significant correlation with any of the explanatory models tested here. The results observed for skull and jaw shape were also manifest when the distances estimated from the residuals of the relationship between shape and centroid were used (Table S8 in Appendix S1). Interestingly, the contribution of genetic structure or resistance distance alone was weak while the model of environmental variables alone was able to explain up to 45% of the total skull

Trait	Populations	Chubut-Santa	Perú	Mendoza	Fuego	Bolivia	Córdoba
Skull shape	Chubut-Santa		***	***	ns	ns	ns
	Perú	0.0259		***	***	ns	***
	Mendoza	0.0142	0.0274		***	***	ns
	Fuego	0.0133	0.0259	0.0199		*	ns
	Bolivia	0.0216	0.0139	0.0231	0.0207		ns
	Córdoba	0.0279	0.0364	0.0275	0.0293	0.0303	
Jaw shape	Chubut-Santa		*	***	ns	***	ns
	Perú	0.0146		*	***	ns	ns
	Mendoza	0.0158	0.0139		***	*	ns
	Fuego	0.0184	0.0221	0.0203		*	ns
	Bolivia	0.0175	0.0161	0.0139	0.0231		ns
	Córdoba	0.0308	0.0276	0.0257	0.0379	0.0303	
Skull size	Chubut-Santa		*	***	*	**	ns
	Perú	0.0468		ns	***	ns	ns
	Mendoza	0.0547	0.0079		***	ns	ns
	Fuego	0.0671	0.1139	0.1218		***	*
	Bolivia	0.0677	0.021	0.013	0.1348		ns
	Córdoba	0.0309	0.0159	0.0238	0.098	0.0368	

TABLE 2 Pairwise divergence between populations of Andean fox in skull shape, jaw shape and skull size. Population differences in skull shape and jaw shape were quantified by calculating the Procrustes distances among populations and the significance was assessed with a permutation test (10,000 permutations). Population differences in skull centroid size were quantified by performing a one-way ANOVA followed by pairwise comparisons using the Tukey post hoc test. Significance levels are given above the diagonal. The Córdoba population shows many non-significant differences due of its small sample size ($N = 2$)

*$p < .05$; **$p < .01$; ***$p < .001$; ns: not significant.

size variation and was the overall best model according to its AIC score (AIC score 2.99 units lower than the highest scoring model but with two parameters fewer; Table 3).

We further analysed the relationships between changes in particular environmental variables and changes in skull size by performing multiple or partial SAR analyses. Out of the 165 skull samples, nine showed imprecise location and thus discarded from the analyses (Table S4 in Appendix S1). We used nine variables that showed the lowest correlation to other variables and that are biologically meaningful for *L. culpaeus* (Table S3 in Appendix S1). The multiple SAR between the individual log-transformed skull centroid size and models including combinations of the nine environmental variables resulted in the best multivariate model including both temperature-related variables (maximum temperature of the warmest month [MTWM] and mean temperature of the wettest quarter [MTWQ]) and precipitation seasonality (PSE) ($df = 150$; $r^2 = .22$; $F = 14.91$; $p < .001$; AIC = −445.37, Figure S5). However, when looking at one variable at a time, the results of the partial SAR analyses indicated that the best overall model (also considering multivariate models) was composed of a single variable, PSE, which explained 21% of the variation in skull centroid size (Table 4). Other single-variable models showed significant results (Table 4), although not the best AIC scores, yet corroborating a contribution of predictor variables associated to temperature (MTWM and MTWQ) and also a contribution brought by a biomass-related variable, AET (Table 4).

Skull size was significantly and positively correlated with two precipitation-related variables (annual precipitation (ANP) and precipitation of the coldest quarter (PCQ)) and with two biomass-related variables (AET and NPP), as revealed by partial SAR analyses (Table 4). Also, skull size was marginally correlated with two temperature-related variables, MTWM and temperature seasonality (TSE). All variables except PCQ showed comparably high AIC scores.

Trait	Model	*df*	*b*	r^2	*p*-value	AIC	ΔAIC
Skull shape	Genetic+Resistance	12		.74	**.006**	−121.07	–
	Genetic structure	13	0.025	.69	**.007**	−120.6	**0.47**
	Resistance	13	0.002	.51	**.007**	−113.69	7.38
Jaw shape	Resistance	13	0.002	.37	.057	−107.04	–
	Genetic+Resistance	12		.41	.243	−106.05	0.99
	Genetic structure	13	0.018	.31	.111	−105.68	1.36
Skull size	Env.+Resist.+Genet.	11		.75	**.009**	−57.26	–
	Environment	13	0.67	.45	**.01**	−54.27	**2.99**
	Resistance	13	0.38	.14	.33	−47.50	9.76
	Genetic structure	13	−0.28	.08	.35	−46.40	10.86

TABLE 3 Multiple regressions on distance matrices (MRM) describing the relationships between the variation of the phenotypic trait of the Andean fox, and the variation of the variables included in the more meaningful models, according to their AIC. ΔAIC refers to the difference relative to the highest (negative) AIC score

Significant values ($p < .05$) are shown in bold type.

TABLE 4 Partial SARs between individual log-transformed Andean fox skull centroid size and environmental variables. Only significant results are shown. ΔAIC refers to the difference relative to the highest (negative) AIC score

Taxon	Category	Variable	*df*	r^2	*b*	*F*	*p*-value	AIC	ΔAIC
Lycalopex culpaeus, *n* = 156	Precipitation	PSE	152	.21	−0.44	40.5	<.001	−445.8	–
	Biomass	AET	152	.04	−0.18	6.72	<.05	−416.1	29.7
	Temperature	MTWM	152	.11	−0.32	18.7	<.001	−427.3	18.5
		MTWQ	152	.04	−0.21	6.92	<.05	−416.2	29.6
L. c. andina, *n* = 26	Precipitation	ANP	22	.15	0.38	4.43	<.05	−71.8	0.1
		PCQ	22	.11	0.35	2.88	<.05	−66.7	5.2
	Biomass	AET	22	.15	0.39	4.56	<.05	−71.9	–
		NPP	22	.14	0.36	3.92	<.05	−71.4	0.5
	Temperature	MTWM	22	.09	−0.31	2.53	.05	−70.0	1.9
		TSE	22	.12	−0.31	3.31	.05	−70.8	1.1

4 | DISCUSSION

Our results highlight the relative importance of neutral and deterministic process in intraspecific phenotypic variation. The multifactorial approach contrasts with most previous attempts to assess the importance of candidate factors in explaining phenotypic change in mammals as they have generally focused on a single factor, most often environmental condition (Medina, Martí, & Bidau, 2007; Sepúlveda et al., 2013). However, some notable attempts have been made to assess the effects of more than one candidate process (e.g. Mullen et al., 2009; Ravinet, Prodöhl & Harrod, 2013; Wang & Summers, 2010).

We identified six genetically differentiated populations in the Andean fox, which correspond well to the described subspecies (Wozencraft, 2005). Importantly, the population structure revealed by the maternally inherited mtDNA was also supported by the nuclear intron data, indicating a small difference between male and female dispersal behaviour. The strong population structure in *L. culpaeus* is remarkable, as most generalist and highly vagile species display weak differentiation (Martinez, Zurano, Molina, & Bidau, 2013). We showed that recent barriers to gene flow are not related to geographical distances between populations but can be explained by environmental resistance, as demonstrated by the out-performance of the IBR over the IBD model. Other studies report that resistance distance generally offers a better explanation for gene flow and population dynamics than geographical distance or least-cost distance (Sexton, Hangartner, & Hoffmann, 2013; Shah & McRae, 2008). These observations are supported by the projections of ENM models into the LGM. The Córdoba population is clearly climatically isolated in the present day, but in the glacial period, there appears to have existed an increase of the climatically potential areas suitable for occupation, facilitating an increase in gene flow with populations from the northern part of the country.

The population differences in skull shape centred on the shape of the zygomatic arch, and on the proportions of the neurocranium (Figure S3 in Appendix S1), two features suggested to be finely moulded through evolution as they participate in key functions (Figueirido et al., 2013). We have found that the population differences in skull shape were only correlated with the genetic structure of populations, supporting the neutral hypothesis. The interpretation is that, variation in skull shape is driven by a relatively long-standing neutral process. The shape of the jaw also showed significant population differences, explained in large part by the development of the coronoid process and the angle and height of the mandibular body (Figure S3 in Appendix S1). These two characteristics are again related to the strength of the bite and to mechanical resistance to break (Figueirido et al., 2013). Here, none of the models tested could explain a significant fraction of the inter-population variation in jaw shape. This raises the possibility that factors not envisaged here might explain the variation. For example, we did not explore local adaptation driven by factors not closely related to environmental variables like the ability to hunt or gather local food items. Also, phenotypic plasticity not strictly related to environmental variables might contribute to population differentiation. It is thus possible that complex interactions among a large number of factors, each of them acting at a low intensity, explain the observed variation. Taken together, our results on inter-population variation in the shape of cranial structures indicate that population divergences can be driven by long-standing genetic isolation and neutral evolution and that other forces may act at a much lower level.

The above conclusions are in apparent contrast with recent work suggesting that adaptation plays a main role in the evolution of skull shape in mammals (Sexton et al., 2013) and particularly in carnivores (Figueirido et al., 2013). However, these studies have been conducted at the interspecific level and the conclusions may not hold true at the intraspecific level where species-specific ecological and life history characteristics may have a strong influence on the processes that drive population phenotypic variation. For instance, *L. culpaeus* is a generalist species capable of using a wide variety of resources, switching from one to another when the abundance of a given prey decreases (Pia, 2013). Accordingly, weak or no local adaptive change in cranial structures is expected. The cranial phenotype of the Andean fox seems to be functionally adequate for a wide range of conditions, in accordance with its generalist ecology. We argue that population differences in ecological niche are too weak to drive significant adaptive changes in cranial structures in this generalist species. This conclusion may not hold true for specialist species.

Nevertheless, some inter-population variation is tolerated in the Andean fox, which we have shown to be driven by neutral evolution.

Probably the most obvious and rapidly evolving phenotypic trait in animals is body size (Martinez, Marti, Molina, & Bidau, 2013; Sookias, Benson, & Butler, 2012). We investigated the determinants of body size in *L. culpaeus* by using skull size as a faithful approximation (Meiri et al., 2005). Skull size showed an increase with increasing latitude, in accordance with Bergmann's rule (Bergmann, 1847). In mammals, the causative factors leading to such a trend at the intraspecific level are a matter of debate. On the one hand, a large body size is believed to be advantageous and positively selected in cold regions because heat loss is more limited in larger than in smaller individuals (Mayr, 1956). On the other hand, this trend could be a phenotypic plasticity response to particular environmental variables. Primary productivity and food abundance have been postulated to be important determinants of animal body size (Medina et al., 2007; Rosenzweig, 1968; Yom-Tov & Geffen, 2006). Because food abundance and temperature are generally highly correlated, the causative forces driving body size changes are still unclear.

Our results indicate that population divergence in skull size can be explained in large part (75% of total variance) by a model combining the effects of environmental variables, resistance distance, and genetic structure. As explained before, resistance distance and genetic structure can be seen as two temporal scales of neutral evolution, with resistance distance corresponding to recent genetic drift and genetic structure reflecting essentially long-term neutral evolution. However, the best overall explanatory model is linked to environment variables (explaining 45% of total variance).

Using multiple and partial SAR analyses, we show that skull size was significantly and negatively correlated with PSE, with actual evapotranspiration (a biomass-related variable) and with temperature-related variables (MTWM and MTWQ). The significant relationship between skull size and temperature-related variables is indicative of local adaptation to temperature, supporting the thermoregulation hypothesis. However, the variables of PSE and biomass (AET) are highly correlated with food abundance and the temporal control of its variation, particularly in semi-arid regions (Guttal & Jayaprakash, 2007), supporting the hypothesis of resource availability. We expect that larger individuals will have an advantage over the smaller ones to exploit available resources, thus being positively selected for leading along the generations, to a positive correlation between size and resource availability. Thus, the relationship between PSE and AET with body size may signal local adaptation. Furthermore, primary productivity (biomass) and food abundance have long been considered as a central determinant of body size (Rosenzweig, 1968), particularly during the growth period of mammalian juveniles (Lindstrom, 1999). Variation in PSE and in biomass-related variables will induce variation in food availability for juveniles, which in turn will cause variation in adult body mass. Then, considering that our macroecological approach impedes controlling individual genetic variation, a possible effect on size derived from phenotypic plasticity cannot be discarded. Thus, our results strongly suggest that three processes—neutral evolution, local adaptation to temperature and food availability and/or phenotypic plasticity—drive skull size and, by extension, body size variation in the Andean fox.

To assess the temporal dimension of the phenotypic response to the effects of environmental variables, we checked if a significant correlation between phenotypic variation and environmental changes was detectable when considering a single lineage rather than the entire species. To achieve this, we analysed the lineage corresponding to the subspecies *L. c. andina*, which inhabits a region restricted in latitude (to reduce the potentially confounding latitudinal effects), yet encompassing many different habitats. Our results indicate, on the one hand, a correlation between skull size variation among individuals and temperature-related variables (TSE and MTWM). We thus concluded that the effects of temperature-driven natural selection are already visible at reduced geographical and time-scales, although marginally supported (Table 4). On the other hand, skull size was significantly and positively correlated with precipitation-related variables (ANP and PCQ) and biomass-related variables (AET and NPP; Table 4), indicating a substantial local adaptation and/or phenotypic plasticity effect. Taken together, these results confirm our previous conclusion stating that local adaptation, without discarding a possible effect of phenotypic plasticity, contributes to skull size variation in this species.

By using multivariate regression analyses employed in spatial ecology, we demonstrated that population phenotypic variation in the Andean fox *L. culpaeus* is driven by phenotypic plasticity, local adaptation and neutral evolution. Neutral evolution is the main factor explaining skull shape variation among populations, while phenotypic plasticity, local adaptation and neutral evolution drive the divergence of skull and body sizes. Whether the conclusions of our pioneering work on a generalist canid species hold true for the majority of mammalian species deserves further examination. Our work offers a methodological framework to test the explanatory power of multiple factors simultaneously.

ACKNOWLEDGEMENTS

We thank editor A. Parmakelist, the anonymous reviewers and M. A. Olalla-Tárraga, F. Perini, S. Lima and G. Correa Costa for helpful discussions. We are grateful to D. Cossios for sharing sequence data and to the following persons and institutions for the access to collection specimens or samples: S. Bogan, Fundación Félix de Azara, Argentina; D. Flores, Museo Argentino de Ciencias Naturales Bernardino Rivadavia, Argentina; D. Verzi, Museo de La Plata, Argentina; M. Diaz and R. Barquez, Museo Miguel Lillio de Ciencias Naturales, Tucumán, Argentina; C. Venegas, Museo Regional de Magallanes, Chile; V. Pérez D'angello and J. Cárcamo, Instituto de la Patogonia, Universidad de Magallanes, Chile;V. Pacheco, Museo de Historia Natural de Lima, Perú; the team of "Las Catalinas", Santa Cruz, Argentina; E. Gallo, Tierra del Fuego National Park; and the Regional Delegations of Patagonia and Regional Delegation of Centre, Argentina. We acknowledge the financial support by: CAPES-REUNI, PE Course of UFRN (to P.M.), Claraz Donation (to J.M.B.) and FNS (grant 31003A_141233 to J.M.B.).

DATA ACCESSIBILITY

1. DNA sequences were deposited in GenBank and the accession numbers are given the online Supporting Information file in Appendix S1.
2. Phylogenetic data: the DNA sequence alignment is available at http://zoology.unige.ch/montoya/
3. Sample locations and museum voucher numbers are presented in the online Supporting Information file in Appendix S1.
4. Input file for inferring the ENM using MAXENT is given in the online Supporting Information file in Appendix S1.

ORCID

Pablo A. Martinez http://orcid.org/0000-0002-5583-3179

REFERENCES

Bergmann, C. (1847). Über die Verhältnisse der Wärmeökonomie der Thiere zu ihrer Grösse. *Göttinger Studien*, *3*, 595–708.

Bidau, C. J., & Martínez, P. A. (2016). Sexual size dimorphism and Rensch's rule in Canidae. *Biological Journal of the Linnean Society*, *119*, 816–830. https://doi.org/10.1111/bij.12848

Burnham, K. P., & Anderson, D. R. (2002). *Model selection and multimodel inference: A practical information-theoretic approach* (2nd ed.). New York: Springer.

Cramer, W. P., & Leemans, R. (2001). Global 30-Year Mean Monthly Climatology, 1930-1960, Version 2.1. Data Set. Oak Ridge National Laboratory Distributed Active Archive Center, Oak Ridge, TN, USA. Retrieved from http://www.daac.ornl.gov.

Davis, M. B., Shaw, R. G., & Etterson, J. R. (2005). Evolutionary responses to changing climate. *Ecology*, *86*, 1704–1714. https://doi.org/10.1890/03-0788

Dupanloup, I., Schneider, S., & Excoffier, L. (2002). A simulated annealing approach to define the genetic structure of populations. *Molecular Ecology*, *11*, 2571–2581. https://doi.org/10.1046/j.1365-294X.2002.01650.x

Excoffier, L., & Lischer, H. E. L. (2010). Arlequin suite ver 3.5: A new series of programs to perform population genetics analyses under Linux and Windows. *Molecular Ecology Resources*, *10*, 564–567. https://doi.org/10.1111/j.1755-0998.2010.02847.x

Figueirido, B., Tseng, Z. J., & Martín-Serra, A. (2013). Skull shape evolution in durophagous carnivorans. *Evolution*, *67*, 1975–1993. https://doi.org/10.1111/evo.12059

Fisher, R. A. (1930). *The genetical theory of natural selection*. Oxford: Clarendon. https://doi.org/10.5962/bhl.title.27468

Fitch, W. T. (2000). Skull dimensions in relation to body size in non-human mammals: The causal basis for acoustic allometry. *Zoology*, *103*, 40–58.

Goslee, S. C., & Urban, D. L. (2007). The ecodist package for dissimilarity-based analysis of ecological data. *Journal of Statistical Software*, *22*, 1–19.

Guttal, V., & Jayaprakash, C. (2007). Self-organization and productivity in semi-arid ecosystems: Implications of seasonality in rainfall. *Journal of Theoretical Biology*, *248*, 490–500. https://doi.org/10.1016/j.jtbi.2007.05.020

Heath, T. A., Hedtke, S. M., & Hillis, D. M. (2008). Taxon sampling and the accuracy of phylogenetic analyses. *Journal of Systematic and Evolution*, *46*, 239–257.

Hijmans, R. J., Cameron, S. E., Parra, J. L., Jones, P. G., & Jarvis, A. (2005). Very high resolution interpolated climate surface ofr global land areas. *International Journal of Climatology*, *25*(15), 1965–1978. https://doi.org/10.1002/(ISSN)1097-0088

Hijmans, R. J., Guarino, L., & Mathur, P. (2012). DIVA-GIS version 7.5. Retrieved from http://www.diva-gis.org/download.

Huelsenbeck, J. P., & Ronquist, F. (2001). MRBAYES: Bayesian inference of phylogenetic trees. *Bioinformatics*, *17*, 754–755. https://doi.org/10.1093/bioinformatics/17.8.754

Imhoff, M. L., Bounoua, L., Ricketts, T., Loucks, C., Harriss, R., & Lawrence, W. T. (2004). Global patterns in human consumption of net primary production. *Nature*, *429*, 870–873. https://doi.org/10.1038/nature02619

Kissling, W. D., & Carl, G. (2008). Spatial autocorrelation and the selection of simultaneous autoregressive models. *Global Ecology and Biogeography*, *17*, 59–71.

Klingemberg, C. P. (2008). MorphoJ. Faculty of Life Sciences, University of Manchester, Manchester. Retrieved from http://www.flywings.org.uk/MorphoJ_page.htm.

Lanfear, R., Calcott, B., Ho, S. Y., & Guindon, S. (2012). Partitionfinder: Combined selection of partitioning schemes and substitution models for phylogenetic analyses. *Molecular Biology and Evolution*, *29*, 1695–1701. https://doi.org/10.1093/molbev/mss020

Lindstrom, J. (1999). Early development and fitness in birds and mammals. *Trends in Ecology and Evolution*, *14*, 343–348. https://doi.org/10.1016/S0169-5347(99)01639-0

Martinez, P. A., Marti, D. A., Molina, W. F., & Bidau, C. J. (2013). Bergmann's rule across the equator: A case study in *Cerdocyon thous* (Canidae). *Journal of Animal Ecology*, *82*, 997–1008. https://doi.org/10.1111/1365-2656.12076

Martinez, P. A., Zurano, J. P., Molina, W. F., & Bidau, C. J. (2013). Applications and implications of phylogeography for canid conservation. *Mastozoologia Neotropical*, *20*, 61–74.

Mayr, E. (1956). Geographical character gradients and climatic adaptation. *Evolution*, *10*, 105–108. https://doi.org/10.1111/j.1558-5646.1956.tb02836.x

Medina, A. I., Martí, D. A., & Bidau, C. J. (2007). Subterranean rodents of the genus Ctenomys (Caviomorpha, Ctenomyidae) follow the converse to Bergmann's rule. *Journal of Biogeography*, *34*, 1439–1454. https://doi.org/10.1111/j.1365-2699.2007.01708.x

Meiri, S., Dayan, T., & Simberloff, D. (2005). Biogeographical patterns in the Western Palearctic: The fasting-endurance hypothesis and the status of Murphy's rule. *Journal of Biogeography*, *32*, 369–375. https://doi.org/10.1111/j.1365-2699.2005.01197.x

Meyers, L. A., & Bull, J. J. (2002). Fighting change with change: Adaptive variation in an uncertain world. *Trends in Ecology and Evolution*, *17*, 551–557. https://doi.org/10.1016/S0169-5347(02)02633-2

Mitchell-Olds, T., Willis, J. H., & Goldstein, D. B. (2007). Which evolutionary processes influence natural genetic variation for phenotypic traits? *Nature Reviews Genetics*, *8*, 845–856. https://doi.org/10.1038/nrg2207

Montoya-Burgos, J. I. (2011). Patterns of positive selection and neutral evolution in the protein-coding genes of *Tetraodon* and *Takifugu*. *PLoS ONE*, *6*(9), e24800. https://doi.org/10.1371/journal.pone.0024800

Mousseau, T. A., Uller, T., Wapstra, E., & Badyaev, A. V. (2009). Evolution of maternal effects: Past and present. *Philosophical Transactions Royal Society B*, *364*, 1035–1038. https://doi.org/10.1098/rstb.2008.0303

Mullen, L. M., Vignieri, S. N., Gore, J. A., & Hoekstra, H. E. (2009). Adaptive basis of geographic variation: Genetic, phenotypic and environmental differences among beach mouse populations. *Proceedings of the Royal Society B*, *276*, 3809–3818. https://doi.org/10.1098/rspb.2009.1146

North, A., Pennanen, J., Ovaskainen, O., & Laine, A.-L. (2011). Local adaptation in a changing world: The roles of gene-flow, mutation, and sexual reproduction. *Evolution*, *65*, 79–89. https://doi.org/10.1111/j.1558-5646.2010.01107.x

Novaro, A. J. (1997). *Pseudalopex culpaeus*. *Mammalian Species*, *558*, 1–8. https://doi.org/10.2307/3504483

Olson, D. M., Dinerstein, E., Wikramanayake, E. D., Burgess, N. D., Powell, G. V. N., Underwood, E. C., ... Kassem, K. R. (2001). Terrestrial ecoregions of the world: A new map of life on Earth. *BioScience*, *51*, 933–938. https://doi.org/10.1641/0006-3568(2001)051[0933:TEOTWA]2.0.CO;2

Phillips, S. J., & Dudik, M. (2008). Modeling of species distributions with Maxent: New extensions and a comprehensive evaluation. *Ecography*, *31*, 161–175. https://doi.org/10.1111/j.0906-7590.2008.5203.x

Pia, M. V. (2013). Trophic interactions between puma and endemic culpeo fox after livestock removal in the high mountains of central Argentina. *Mammalia*, 1–11.

Pollock, D. D., Zwickl, D. J., McGuire, J. A., & Hillis, D. M. (2002). Increased taxon sampling is advantageous for phylogenetic inference. *Systematic Biology*, *51*, 664–671. https://doi.org/10.1080/10635150290102357

R Core Team (2015). *R: A language and environment for statistical computing*. Vienna, Austria: R Foundation for Statistical Computing.

Rangel, T. F., Diniz-Filho, J. A. F., & Bini, L. M. (2010). SAM: A comprehensive application for spatial analysis in macroecology. *Ecography*, *33*, 46–50. https://doi.org/10.1111/j.1600-0587.2009.06299.x

Ravinet, M., Prodöhl, P. A., & Harrod, C. (2013). Parallel and nonparallel ecological, morphological and genetic divergence in lake-stream stickleback from a single catchment. *Journal of Evolutionary Biology*, *26*, 186–204.

Raymond, M., & Rousset, F. (1995). GENEPOP (Version-1.2) – population-genetics software for exact tests and ecumenicism. *Journal of Heredity*, *86*, 248–249. https://doi.org/10.1093/oxfordjournals.jhered.a111573

Rohlf, F. J. (2010). TpsDig, ver 2.16. Department of Ecology and Evolution, State University of New York, Stony Brook. Retrieved from http://life.bio.sunysb. edu/morph/.

Rosenzweig, M. L. (1968). The strategy of body size in mammalian carnivores. *American Midland Naturalist*, *80*, 299–315. https://doi.org/10.2307/2423529

Rousset, F. (1997). Genetic differentiation and estimation of gene flow from F-statistics under isolation by distance. *Genetics*, *145*, 1219–1228.

Rundle, H. D., & Nosil, P. (2005). Ecological speciation. *Ecology Letters*, *8*, 336–352. https://doi.org/10.1111/j.1461-0248.2004.00715.x

Segura, V., & Prevosti, F. J. (2012). A quantitative approach to the cranial ontogeny of Lycalopex culpaeus (Carnivora: Canidae). *Zoomorphology*, *131*, 79–92. https://doi.org/10.1007/s00435-012-0145-4

Sepúlveda, M., Oliva, D., Duran, L. R., Urra, A., Pedraza, S. N., Majluf, P., ... Crespo, E. A. (2013). Testing Bergmann's rule and the Rosenzweig hypothesis with craniometric studies of the South American sea lion. *Oecologia*, *171*, 809–817.

Sexton, J. P., Hangartner, S. B., & Hoffmann, A. A. (2013). Genetic isolation by environment or distance: Which pattern of gene flow is most common? *Evolution*, *68*(1), 1–15. https://doi.org/10.1111/evo.12258

Shah, V. B., & McRae, B. H. (2008). Circuitscape: A tool for landscape ecology. In G. Varoquaux, T. Vaught & J. Millman (Eds.). Proceedings of the 7th Python in Science Conference (SciPy 2008). pp. 62–66.

Slater, G. J. (2015). Iterative adaptive radiations of fossil canids show no evidence for diversity-dependent trait evolution. *Proceedings of the National Academy of Sciences*, *112*, 4897–4902.

Sookias, R. B., Benson, R. B. J., & Butler, R. J. (2012). Biology, not environment, drives major patterns in maximum tetrapod body size through time. *Biology Letters*, *8*, 674–677. https://doi.org/10.1098/rsbl.2012.0060

Stamatakis, A. (2006). RAxML-VI-HPC: Laximum likelihood-based phylogenetic analyses with thousands of taxa and mixed models. *Bioinformatics*, *22*, 2688–2690. https://doi.org/10.1093/bioinformatics/btl446

Wagner, A. (2008). Neutralism and selectionism: A network-based reconciliation. *Nature Reviews Genetics*, *12*, 965–974. https://doi.org/10.1038/nrg2473

Wang, I. J., & Summers, K. (2010). Genetic structure is correlated with phenotypic divergence rather than geographic isolation in the highly polymorphic strawberry poison-dart frog. *Molecular Ecology*, *19*, 447–458. https://doi.org/10.1111/j.1365-294X.2009.04465.x

Wayne, R. K., Geffen, E., Girman, D. J., Koepfli, K. P., Lau, L. M., & Marshall, C. R. (1997). Molecular systematics of the Canidae. *Systematic Biology*, *46*, 622–653. https://doi.org/10.1093/sysbio/46.4.622

Wozencraft, W. C. (2005). Order Carnivora. In D. E. Wilson & D. M. Reeder (Eds.), *Mammal species of the World: A taxonomic and geographical reference* (pp. 532–628). Baltimore: Johns Hopkins University Press.

Yom-Tov, Y., & Geffen, E. (2006). The determination of mammal body size: Ambient temparature or food? *Oecologia*, *148*, 213–218. https://doi.org/10.1007/s00442-006-0364-9

Zurano, J. P., Martinez, P. A., Hernández, J. C., Montoya-Burgos, J. I., & Costa, G. C. (2017). Morphological and ecological divergence in South American canids. *Journal of Biogeography*, *44*(4), 821–833. https://doi.org/10.1111/jbi.12984

BIOSKETCH

Pablo A. Martinez is professor of Universidade Federal do Sergipe in Brazil. His research is focused in understanding the historical and ecological process that drive the spatial and temporal variations of body size, sexual dimorphism, diversification rate and chromosomal diversity of animals.

Author contributions: P.A.M., C.J.B. and J.M.B conceived the ideas. P.A.M., M.V.P and J.M.B collected the morphological data. P.A.M., I.A.B. and J.M.B performed the molecular analyses. All authors contributed to the discussion and final writing of the manuscript.

SUPPORTING INFORMATION

Additional Supporting Information may be found online in the supporting information tab for this article.

How to cite this article: Martinez PA, Pia MV, Bahechar IA, Molina WF, Bidau CJ, Montoya-Burgos JI. The contribution of neutral evolution and adaptive processes in driving phenotypic divergence in a model mammalian species, the Andean fox *Lycalopex culpaeus*. *J Biogeogr*. 2018;00:1–12. https://doi.org/10.1111/jbi.13189